Pluripotency of mouse spermatogonial stem cells maintained by IGF-1- dependent pathway

Yen-Hua Huang,[*,†,‡,1] Cheng-Chieh Chin,[*,†] Hong-Nerng Ho,[§,‖] Chuan-Kai Chou,[#] Chia-Ning Shen,[,‡‡] Hung-Chih Kuo,[**,††] Tsai-Jung Wu,[*,†] Yu-Chih Wu,[*,†,‡‡] Yu-Ching Hung,[#] Chih-Cheng Chang,[*,†] and Thai-Yen Ling[¶,1]**

[*]Department of Biochemistry, [†]Graduate Institute of Medical Sciences, School of Medicine, and [‡]Center for Reproductive Medicine, Taipei Medical University Hospital, Taipei Medical University, Taipei, Taiwan; [§]Division of Reproductive Endocrinology and Infertility, Department of Obstetrics and Gynecology, College of Medicine and Hospital, National Taiwan University, Taipei, Taiwan; [‖]Graduate Institute of Immunology and [¶]Institute of Pharmacology, College of Medicine, National Taiwan University, Taipei, Taiwan; [#]National Laboratory Animal Center, National Applied Research Laboratories, Taipei, Taiwan; **Stem Cell Program, Genomic Research Center, and [††]Institute of Cellular and Organismic Biology, Academia Sinica, Taipei, Taiwan; and [‡‡]Graduate Institute of Life Sciences, National Defense Medical Center, Taipei, Taiwan

ABSTRACT **Recent studies indicate that neonatal spermatogonial stem cells (SSCs) possess pluripotency. However, the mechanisms that regulate the pluripotent differentiation capacity of SSCs remain unclear. Here, we describe a new method to clonally derive pluripotent SSCs from neonatal mouse testis. By coculturing with testicular stromal cells, SSCs can be maintained and expanded in serum-free conditions. Unlike endogenous SSCs, these *in vitro* expanded SSCs showed strong alkaline phosphatase (AP) activity and displayed characteristics of embryonic stem cells and primordial germ cells, which were therefore designated as AP^+ germline stem cells (AP^+GSCs). The pluripotency of AP^+GSCs was confirmed by *in vitro* differentiation toward hepatic and neuronal lineages and formation of embryonic chimeras after injection into blastocysts. Further investigation revealed that insulin-like growth factor-1 (IGF-1) secreted from Leydig cells was a key factor involved in maintaining the pluripotency of AP^+GSCs. The blockage of IGF-1 receptor phosphorylation and its downstream PI3K pathway by PPP or LY294002 dramatically reduced their AP activity and expression of pluripotent genes, such as *Oct-4*, *Blimp1*, and *Nanog*. In conclusion, the present study demonstrated that IGF-1 secreted by testicular Leydig cells plays an important role in maintaining the pluripotency of SSCs in culture, which provides an insight into the molecular mechanism underlying germ cell pluripotency.—Huang, Y.-H., Chin, C.-C., Ho, H.-N., Chou, C.-K., Shen, C.-N., Kuo, H.-C., Wu, T.-J., Wu, Y.-C., Hung, Y.-C., Chang, C.-C., Ling, T.-Y. Pluripotency of mouse spermatogonial stem cells maintained by IGF-1-dependent pathway. *FASEB J.* 23, 2076–2087 (2009)**

Key Words: germline stem cells · stem cell-microenvironment interaction · Leydig cells · serum-free culture · cell signaling

Germline stem cells (GSCs), including primordial germ cells (PGCs; the germ cell precursors), gonocytes (transient prospermatogonia), and spermatogonial stem cells (A_{single} SSCs), are cells that are able to self-renew and differentiate into mature sperm (1). In addition to postfertilization development, the pluripotency of GSCs has been shown by their ability to form teratomas in testis or ovary (2). Recent studies (3) have demonstrated that p53-knockout neonatal SSCs respond to culture conditions and acquire pluripotency. However, the lack of understanding regarding the regulatory mechanisms of pluripotency often results in an inefficient generation of pluripotent stem cells from wild-type neonatal mouse testis (3). The use of serum-containing medium for the generation of multipotent adult germline stem cells (maGSCs) from testis of Stra8-GFP transgenic mice also limits the possibility of identifying specific endocrine factors that mediate the pluripotency of SSCs (4).

Undefined components in certain batches of serum (5) may limit the ability of SSCs to acquire pluripotency or may affect the maintenance of stem cell pluripotency. To circumvent the serum factors, there have been several attempts to cultivate mouse SSCs *in vitro* in serum-free conditions with mouse embryonic fibroblast feeders (6–10). However, in these studies, utilizing these nonphysiologically relevant feeders resulted in loss of spermatogonial potency in culture (8) and selective outgrowth of differentiated sperm cells (A_4–A_{32} alignment; ref. 10). Therefore, the medium was supplemented with selected exogenous cytokines to support the self-renewal growth of GSCs. With the use

[1] Correspondence: Y.-H.H., Department of Biochemistry, Graduate Institute of Medical Sciences, School of Medicine, Taipei Medical University, Taipei, Taiwan. E-mail: rita1204@tmu.edu.tw; T.-Y.L., Institute of Pharmacology, College of Medicine, National Taiwan University, Taipei, Taiwan. E-mail: tyling@ntu.edu.tw

doi: 10.1096/fj.08-121939

0892-6638/09/0023-2076 © FASEB

of this approach, glial cell line-derived neurotropic factor (GDNF) was the first cytokine demonstrated to be directly involved in regulating the self-renewal of mouse SSCs (8, 11). GDNF was able to activate PI3K/Akt and Src kinase-mediated signaling pathways, which led to the up-regulation of the self-renewal-associated transcription factors *Bcl6b*, *Erm*, and *Lhx1* (12, 13). However, the genes that regulate pluripotency or self-renewal like *Oct-4* and *Plzf* were not affected by GDNF treatment (13). These observations suggest that factors involved in mediating pluripotency of SSCs have yet to be identified.

In the present study, we established a serum-free culture system using testicular stromal cells as feeders to clonally derive pluripotent SSCs from wild-type neonatal mouse testes. These cells showed strong alkaline phosphatase (AP) activity and displayed characteristics of embryonic stem cells (ESCs) in which they were able to differentiate into neuron-like cells, hepatocyte-like cells, and c-kit$^+$ germ cells *in vitro* and to form embryonic chimeras after injection into blastocysts. AP$^+$GSCs could also contribute to spermatogenesis after transplantation to recipient testes pretreated with bulsufan. Most importantly, in addition to the role of GDNF in SSC self-renewal, we further identified a paracrine factor, insulin-like growth factor-1 (IGF-1), which was secreted by Leydig cells, as a key factor that regulated the self-renewal growth and pluripotency of SSCs. These findings led to exploration of germ cell pluripotency.

MATERIALS AND METHODS

Cultivation of mouse AP$^+$GSCs in serum-free culture medium

Newborn ICR or enhanced green fluorescence protein (EGFP) mice [FVB/NCrl-*Tg*(*Pgk1-EGFP*)3Narl], which ubiquitously expressed EGFP in all tissues, were obtained from National Laboratory Animal Center and National Applied Research Laboratories (Taipei, Taiwan). Testes from 0–2 days postpartum (dpp) newborn ICR or EGFP mice were collected and briefly washed in Hank's buffer (Gibco-BRL, Grand Island, NY, USA) containing penicillin (100 U/ml) and streptomycin (100 μg/ml) and then treated with 0.1% protease type-XIV (Sigma, St. Louis, MO, USA) in MCDB-201 medium (Sigma) at 4°C for 16–20 h. Digested tissues were transferred to Joklik's suspension modified minimum essential medium (SMEM; Sigma) containing 10% FCS and filtrated through a 70 μm nylon cell strainer to remove the cell debris. Basically, one testis could yield ~1.5×10^5 cells. Total testicular cells were resuspended in the basic culture medium (BM) composed of MCDB-201 supplemented with 1× ITS (insulin, transferrin, selenium) and 10 ng/ml of epidermal growth factor (EGF; Gibco-BRL). Testicular cells were seeded at a density of 8×10^4 cells/cm^2 in a laminin-coated culture plate, and cultivated in an incubator at 37°C, 5% CO_2 for 7 d.

AP activity assay

Clump GSC colonies in serum-free medium were fixed with 3.7% paraformaldehyde for 30 min at room temperature. The AP activity of these GSC colonies was measured with an AP detection kit according to the manufacturer's instructions (Chemicon, Chandlers Ford, UK).

RNA isolation and RT-PCR

The total RNA of AP$^+$GSC colonies was extracted with the RNeasy Micro kit (Qiagen, Valencia, CA, USA), according to the manufacturer's instructions. Three micrograms of total RNA was used to synthesize cDNA with random primer (Invitrogen, Carlsbad, CA, USA). The cDNA synthesis was performed at 50°C for 50 min in a final volume of 20 μl, according to the manufacturer's instructions for Superscript III reverse transcriptase (Invitrogen). The PCR was conducted with PlatinumTaq polymerase (Invitrogen), and the RT-PCR amplifications were titrated to be within a linear range of amplification. Primer sequences and annealing temperature are listed in Supplemental Table 1. *Gapdh* mRNA was used as an internal control. PCR products were separated by agarose gel electrophoresis, and the DNA bands were visualized with ethidium bromide under ultraviolet light. The RT-PCR analysis of at least three independent cultures was performed for all experiments.

Immunostaining

For detection of Oct-4 expression in primary culture cells, the cells were fixed in methanol:acetone (1:1) at room temperature for 10 min. For other antigens, the cells were fixed with 4% paraformaldehyde at room temperature for 30 min. After fixation, the cells were rinsed with PBS twice and then treated with PBS containing 0.05% Tween-20 (PBST) at room temperature for 10 min and blocked with BSA (5 mg/ml) in PBST for 1 h at room temperature. The cells were then incubated at 4°C overnight with the following antibodies: anti-Oct-4 (sc-9081; Santa Cruz Biotechnology, Santa Cruz, CA, USA), anti-CD29 (clone 9EG7), anti-CD49f (clone GoH3), anti-CD31 (clone MEC13.3), anti-CD34 (clone RAM34; all from BD Biosciences, San Jose, CA, USA), anti-c-kit (CD117, Clone YB5.B8, BD Biosciences), anti-SSEA-1 (clone MC-480; Chemicon), anti-IRα (sc-710) and anti-IGF-1Rα (sc-7952) (Santa Cruz Biotechnology), anti-α-SMA (A-2547, Sigma, for myoid cells), anti-CYP11A1 (sc-18043, Santa Cruz Biotechnology, for Leydig cells), anti-MIS (sc-6886, Santa Cruz Biotechnology, for Sertoli cells), and anti-IGF-1 (sc-9013, Santa Cruz Biotechnology). The nuclei of all cells were counterstained with DAPI (Sigma). All cells were covered with an antifading reagent (Vector Laboratories, Burlingame, CA, USA) and analyzed with a fluorescence microscope (Olympus, Melville, NY, USA). For confocal spectroscopic fluorescence, testicular cells were seeded and grew on the cover glasses for 7 d. The forming AP$^+$GSC colonies were fixed, blocked, and immunoprobed with specific antibodies. All cells were covered with antifading reagent and analyzed with a confocal laser scanning microscope (Leica, Hercules, CA, USA). Neural-lineage cell types, hepatocytes, and germ cell differentiation of AP$^+$GSCs were demonstrated using immunostaining. The differentiated cells were fixed in 4% paraformaldehyde for 30 min at room temperature, and then they were incubated with 5% normal serum for 1 h. After the blocking process, cells were incubated with primary antibody at 4°C overnight. Antibodies used were: anti-MAP2 (for neuron, clone 5F9; UBI, Lake Placid, NY, USA), anti-O4 (for oligodendrocytes, MAB345; Chemicon), anti-glial fibrillary acidic protein (for astrocyte, GFAP, clone G-A-5; Sigma), anti-α-fetoprotein (anti-AFP, for hepatocytes, A0008; DakoCytomation, Carpinteria, CA, USA), or anti-c-kit (CD117, clone YB5.B8; BD Biosciences). Specific labeling for the primary antibod-

ies was detected with Cy3 and/or FITC-conjugated secondary antibodies (Jackson ImmunoResearch, West Grove, PA, USA). The AP^+GSCs were mounted on slides using Vectashield mounting medium (Vector Laboratories), and the staining was examined using epifluorescence microscopes (Olympus).

For immunohistochemical staining, the cyrosection slides of d 18 embryonic chimeras were probed with anti-GFP antibodies (Invitrogen) for microscope analysis or colocalized with CD31 (clone MEC13.3, BD Biosciences), cytokeratin 14 (clone LL002; Novocastra, Newcastle, UK), and AFP (DakoCytomation) by confocal laser scanning microscope (Leica).

Differentiation and proliferation of the AP^+GSCs *in vitro*

For neuron-lineage differentiation, the AP^+GSC colonies were transferred to gelatin (1 mg/ml)-coated plates and treated with trans-retinoic acid (Sigma, 5 μM) combined with 10% FBS-containing BM for 2 wk. For hepatocyte induction, the AP^+GSC colonies were digested into single cells and treated with acidic fibroblast growth factor (aFGF; 20 ng/ml) and basic fibroblast growth factor (bFGF; 10 ng/ml; both from Peprotech, Rocky Hill, NJ, USA) in 15% FBS-IMDM, 2 mM L-glutamine (Sigma), 300 μM monothioglycerol (Sigma) for 2 d, followed by HGF (10 ng/ml; R&D Systems, Minneapolis, MN, USA) treatment for another 2 d. The cells were then incubated with Oncostanin M (10 ng/ml), dexamethasone (100 nM; both from R&D Systems), and 1× ITS supplement (Invitrogene) for the next 2 d (14). For germ cell differentiation, the AP^+GSC colonies were transferred to an uncoated culture plate and incubated with BM containing 10% FBS and stem cell factor (10 ng/ml; Peprotech) for 10 d. To test the PGC potential of retinoic acid-stimulated cell proliferation, the AP^+GSC colonies were digested by collagenase and reseeded on the BM-conditioned methylcellulose soft agars. The medium was supplemented with trans-retinoic acid in concentrations of 0, 0.5, and 1 μM for 10 d to stimulate the proliferation of AP^+GSCs. The colonies were counted for statistical analysis.

Testis transplantation and chimera formation

Functional transplantation of the EGFP-AP^+GSCs to recipient testis was performed according to a previous report (15). For chimera formation, 5 to 10 EGFP-AP^+GSCs were injected into the blastocoels of 3.5 days postcoitum (dpc) blastocysts from C57BL/6 mice using a piezo-driven micromanipulator (Prime Tech, Tsuchiura, Japan). The blastocysts were returned to the uteri of 2.5 dpc pseudo-pregnant CByB6F1 foster mothers on the day of microinjection. The d 18 embryonic chimeras were fixed in 4% paraformaldehyde and frozen in Tissue-Tek OCT compound (Cryochrome; Shandon, Pittsburgh, PA, USA) for cyrosection and anti-GFP immunostaining. Newborn d 4 chimeras were subjected to noninvasive *in vivo* live fluorescence imaging by image visualization and infrared spectroscopy (IVIS Imaging System, 200 Series; Caliper Life Science, Xenogen, Alameda, CA, USA). Three-week-old chimeras were killed to get organ tissues. The tissues were fixed, embedded, and sectioned for GFP immunostaining.

Effect of exogenous factors on AP^+GSC colony formation

Exogenous factors, such as EGF, insulin, IGF-1, selenium, and transferrin, as well as anti-insulin receptor antibodies (αIR, sc-710; Santa Cruz Biotechnology), anti-IGF-1 receptor antibodies (αIR3; Calbiochem, Darmstadt, Germany), rabbit and mouse IgG (Jackson ImmunoResearch), PPP (cyclolignan picropodophyllin; Calbiochem), and LY294002 (Cell Signaling, Danvers, MA, USA), were added to the medium, and the GSCs were cultivated at 37°C, 5% CO_2 for 7 d. After 7 d of cultivation, the AP activity of GSC colonies under different experimental condition was determined. The AP^+GSC colonies were counted for statistical analysis.

Cytokine array analysis

The endocrine factors in the testicular-stromal niche coculture system were examined by mouse cytokine antibody array analysis (AAM-CYT-4–4; RayBiotech, Norcross, GA, USA). Briefly, the array membranes were incubated in blocking buffer at room temperature for 30 min and then incubated with the collected MCDB201 and d 3-conditioned medium (D3-CM) at room temperature for 1–2 h. After incubation, the array membrane was washed at room temperature with gentle shaking. The membranes were then incubated with primary biotin-conjugated antibodies at room temperature for 1–2 h, washed several times, and incubated with horseradish perioxidase (HRP)-conjugated streptavidin for 2 h at room temperature. The array membranes were then washed and exposed to X-ray films.

Western blotting

NCCIT cells and AP^+GSC colonies under different culture conditions were collected and lysed in reducing 2× Laemmli sample buffer. The cell lysates were subjected to 10% SDS-PAGE and then transferred to a PVDF membrane for Western blot analysis. Monoclonal anti-phosphoAkt (Ser-473, anti-Akt, Cell Signaling, 1:1000) and polyclonal anti-Oct-4 antibodies (Santa Cruz Biotechnology, 1:1000) were used as the primary antibody, and HRP-conjugated anti-mouse/rabbit IgG (1:2000) served as the secondary antibody. The enzyme activity of HRP was detected by the ECL system according to the manufacturer's instructions (Amersham Pharmacia Biotechnology, Little Chalfont, UK).

Statistical analysis

All experiments were repeated at least 3 times with different individual samples. Data are expressed as mean ± SD. Difference in means was assessed by one-way ANOVA, followed by the Tukey-Kramer multiple comparisons test.

RESULTS

Generation of $AP^+Oct\text{-}4^+$ GSC colonies in serum-free cultures utilizing feeder cells derived from testicular stroma

To establish a physiologically relevant culture environment for growing GSCs, we initially cocultivated the whole testicular cells in a selective serum-free culture system. Different coating materials, including gelatin, collagen I and IV, and laminin, were tested to find the optimal conditions for selection of niche cells. In our culture system, the addition of laminin was shown to best support AP^+GSC colony formation. As shown in **Fig. 1*A***, the GSC colonies were tightly packed in clump morphology, similar to PGCs and embryonic germ cells (Fig. 1*Aai*; also see Supplemental Fig. 1 and ref. 16). Unlike SSCs, which had weak AP activity (3, 8), these

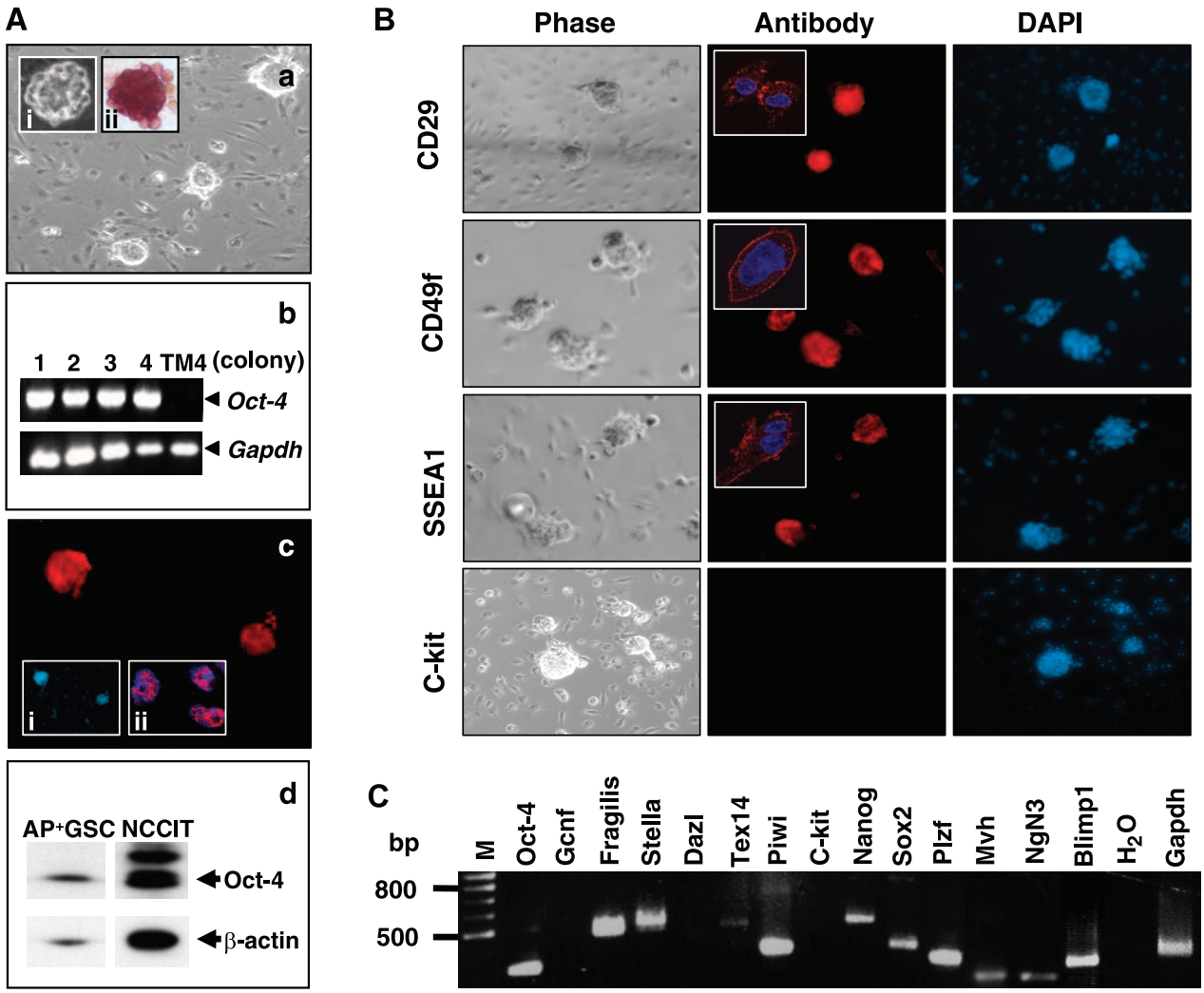

Figure 1. Generation and characterization of the AP$^+$GSC colonies. *A*) Clump colonies were formed when germ cells were cocultured with testicular stroma cells on laminin-coated culture plates (*a*; phase image, *i*); these colonies showed strong AP activity (*ii*). *Oct-4* expression in each AP$^+$GSC colony was analyzed by RT-PCR; TM4 (Sertoli cell line) served as a negative control (*b*). AP$^+$GSC colony cells showed positive immunostaining for Oct-4 (*c*); DAPI staining (*i*); nuclear colocalization of Oct-4 transcription factor and DAPI in each AP$^+$GSC (*ii*). Oct-4 protein expression of AP$^+$GSC colonies was further demonstrated by Western blot. NCCIT cells were used as a positive control (*d*). *B*) Oct-4$^+$AP$^+$GSC colonies showed expression of GSC-associated cell surface markers including integrin β1 (CD29), integrin α6 (CD49f), and SSEA-1. Insets: cell surface expression of marker proteins in each AP$^+$GSC (confocal images). DAPI indicates location of cell nuclei. C-kit shows negative immunostaining. *C*) Gene expression profile of AP$^+$GSC colonies. Primer sequences of genes are shown in Supplemental Table 1.

GSC colonies showed strong AP activity similar to the PGC activity (Fig. 1*Aaii*). We tentatively designated these GSCs as AP$^+$GSCs. RT-PCR demonstrated that the AP$^+$GSC colonies expressed the *Oct-4* gene. *Oct-4* mRNA was expressed in each of the AP$^+$GSC colonies (Fig. 1*Ab*); C-kit was not expressed in the colonies (not shown). The expression of Oct-4 protein in colonies was demonstrated by immunostaining and Western blotting (Fig. 1*Ac, d*). Figure 1*Ac* shows the specific nuclear Oct-4 expression of the AP$^+$GSCs. Figure 1*Aci* shows a DAPI image. The specific nuclear expression of Oct-4 protein in each AP$^+$GSC was further demonstrated by immunostaining and colocalization with DAPI, as shown by confocal microscopy (Fig. 1*Acii*). Oct-4 protein expression in the AP$^+$GSCs was also demonstrated by Western blotting. NCCIT cells (seminoma-embryonal carcinoma cells, which dominantly express Oct-4 protein in the nucleus) were used as a positive control (Fig. 1*Ad*).

Characterization of the AP$^+$ GSC colonies

To characterize the AP$^+$ GSC colonies, the colony cells were immunostained for specific cell surface markers. As shown in Fig. 1*B*, these AP$^+$ GSCs were positively immunostained with GSC-related cell surface markers, including CD29 (integrin β_1, GSC, and ESC marker); CD49f (integrin α_6, GSC, and ESC marker); and notably, embryonic stem cell marker SSEA-1 (stage specific embryonic antigen-1, ESC marker). These marker proteins were expressed in the cytoplasm as well as on the cell surface of each AP$^+$GSC (confocal images in in-

sets). The AP$^+$GSC colonies did not show positive C-kit staining (C-kit panel). Staining for CD31 and CD34 was also negative (not shown). The gene expression profile of these AP$^+$GSC colonies was assessed by RT-PCR (Fig. 1*C*). The colonies expressed *Oct-4*, *Nanog*, and *Sox2* (for ESCs); *Blimp1*, *Fragilis*, *Stella*, and *Mvh* (for PGCs); and *Piwi*, *Plzf*, *C-Ret*, and *Ngn-3* (for SSCs). There was very weak expression of the differentiation germ cell markers *Dazl* and *Tex14* and no expression of *Gcnf* (*Oct-4* suppressor factor) or *c-kit* (differentiated germ cells; Fig. 1*C*). The AP$^+$GSC (AP$^+$Oct-4$^+$c-kit$^-$) colonies accounted for ~0.2% of all testicular cells.

ESC/PGC characteristics of the AP$^+$GSC colony cells

Given that the AP$^+$GSC colonies had gene expression patterns similar to those of ESCs and/or PGCs, we next compared the characteristics of the AP$^+$GSC colonies with those of ESCs/PGCs. As shown in **Fig. 2*A***, the AP activity of the GSCs was similar to that of ESCs (Fig. 2*Aa*, *b*). Further analysis by quantitative real-time PCR showed that the *Oct-4* mRNA level of the AP$^+$GSCs was ~70% that of ESCs (Fig. 2*Ac*). The AP$^+$GSC colonies also showed PGC-like characteristics, such as colony cell migration (Fig. 2*Ba*, *b*) and retinoic acid-stimulated cell proliferation (Fig. 2*Bc*) (17). The gene expression profile of the ESCs and AP$^+$GSCs was further analyzed by RT-PCR. As shown in Fig. 2*C*, the colonies not only expressed SSC-related genes (*c-Ret* and *Ngn3*) but also expressed genes of the ESCs (*Oct-4*, *Nanog*, *Sox2*, and *Eras*) and PGCs (*Oct-4*, *Blimp 1*, *Fragilis*, *Stella*, and *Mvh*). These results suggest that AP$^+$GSC colony cells possess pluripotent potential.

Differentiation potential of AP$^+$GSC colonies *in vitro*

Because of the similar characteristics of AP$^+$GSC colonies and ESCs/PGCs, we examined the differentiation potential of the AP$^+$GSC colonies *in vitro*. As shown in **Fig. 3**, the AP$^+$GSC colonies formed neurons (Fig. 3*A*, MAP2$^+$ staining), astrocytes (Fig. 3*B*, GFAP$^+$ staining), and oligodendrocytes (Fig. 3*C*, O4$^+$ staining) under retinoic acid treatments. Furthermore, AP$^+$GSCs have the differentiation plasticity to form hepatocyte-like cells (Fig. 3*D*, AFP$^+$ staining, solid arrowhead). These observations suggested AP$^+$GSCs have multipotent differentiation capability *in vitro*. The positive and negative controls of the antibodies used for immunostaining are shown in Supplemental Fig. 2.

Contribution of AP$^+$GSCs to spermatogenesis and normal embryonic development

To address whether AP$^+$GSCs possess germ cell differentiation capability, we first found that treatment of stem cell factor would be able to induce AP$^+$GSCs or

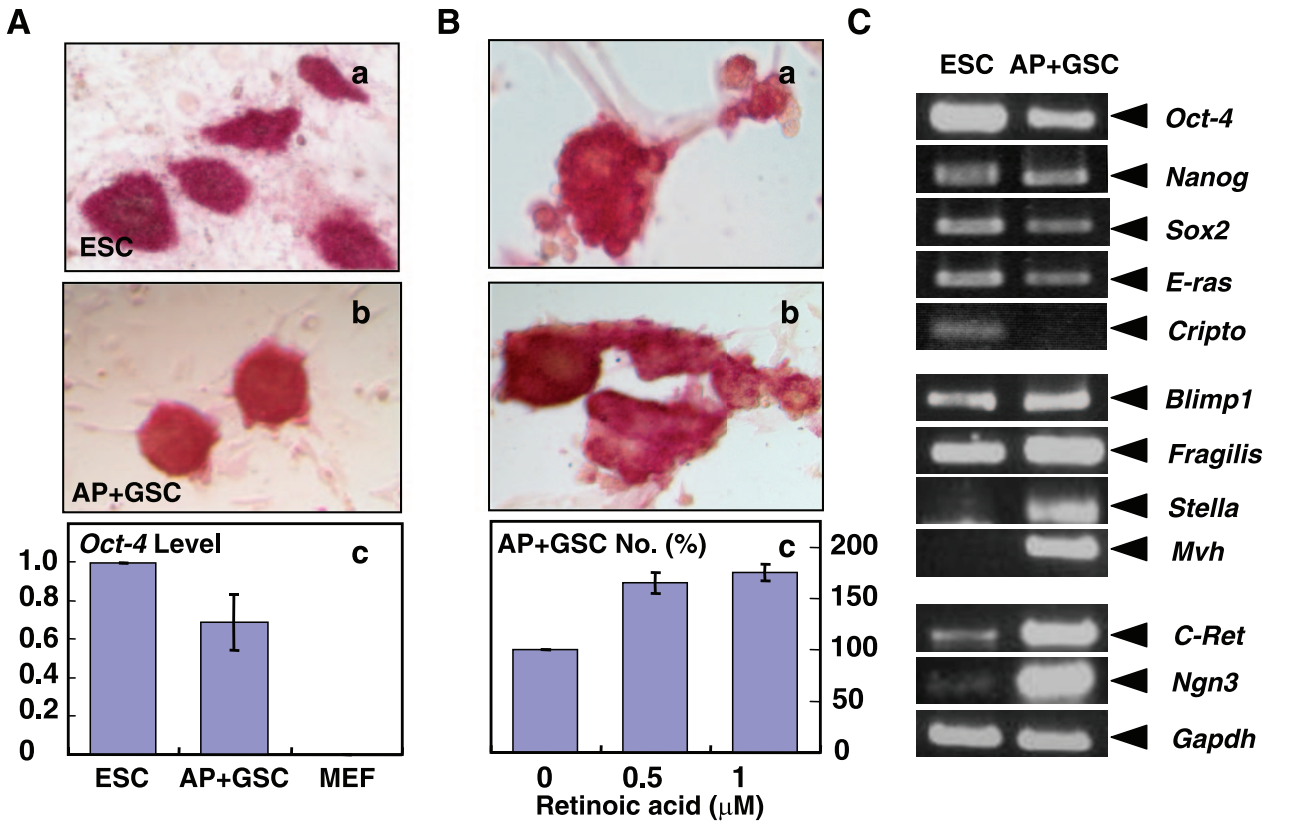

Figure 2. ES/PGC characteristics of AP$^+$GSC colony cells. *A)* Comparison of AP activity (*a*, *b*) and relative *Oct-4* expression level (*c*) between mouse ESCs and AP$^+$GSCs. *B*) PGC-like cell migration (*a*, *b*) and trans-retinoic acid (0, 0.5, and 1 μM)-stimulated cell proliferation (*c*) of AP$^+$GSCs. *C*) Difference in gene expression between mouse ESCs and AP$^+$GSCs.

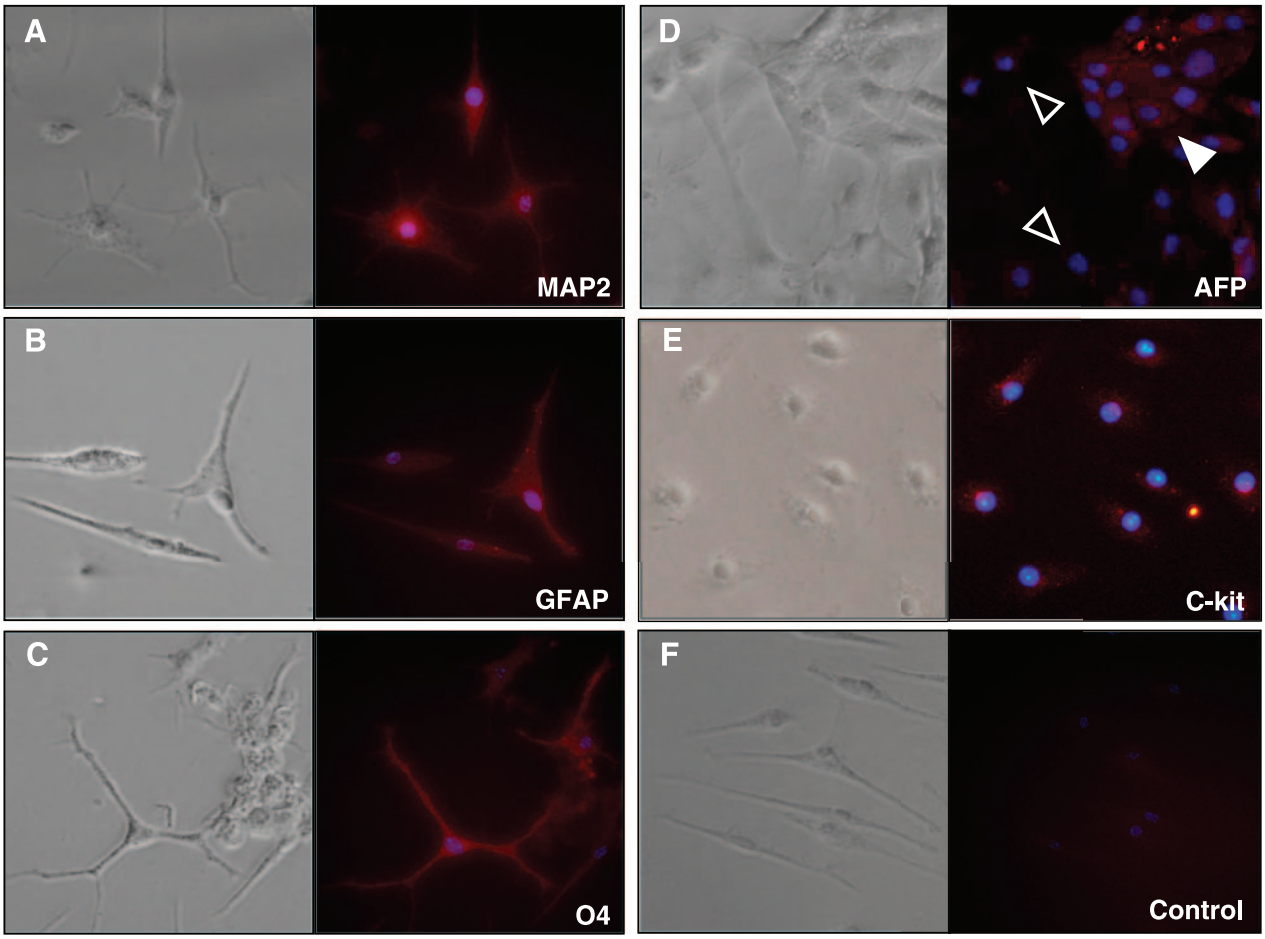

Figure 3. Differentiation potential of AP$^+$GSC colonies *in vitro*. AP$^+$GSC colonies were tested for their pluripotent ability by *in vitro* induction of differentiation. Images show expression of neuronal-lineage cells, including neuron cells (*A*; MAP2$^+$), astrocytes (*B*; GFAP$^+$), oligodendrocytes (*C*; O4$^+$), hepatocytes (*D*; AFP$^+$), and differentiated germ cells (*E*; c-kit$^+$). Cy3-conjugated anti-rabbit IgG was used as a control (*F*). AFP$^+$ cells (solid arrowhead) and AFP$^-$ cells (open arrowheads) of the AP$^+$GSC-derived hepatocyte-like cells are indicated (*D*).

EGFP$^+$ AP$^+$GSCs to differentiate into c-kit$^+$ germ cell precursors *in vitro* (Fig. 3*E*, c-kit$^+$ staining; also see Supplemental Fig. 3*A*). The *in vivo* germ cell differentiation potential of the AP$^+$GSC colony cells was initially investigated by direct testis transplantation, since the colony cells were germ cell oriented (15). The EGFP-AP$^+$GSC colony cells were transplanted into one testis of bulsufan-treated FVB mice (**Fig. 4*A***). Eight weeks after transplantation, the recipient mice were euthanized to check the testis size and spermatogenic reconstitution. As shown in Fig. 4*Aa*, the gross morphology of the transplanted testis (TT) showed a larger size than the untransplanted testis (UT), suggesting the successful reconstitution of the transplanted EGFP-AP$^+$GSCs in TT. Histological staining confirmed that the UT lost the germ cells (Fig. 4*Ab*). In some bulsufan-treated seminiferous tubules, spermatogenesis was recoverable (Fig. 4*Ac*). However, these cells showed negative immunostaining with anti-GFP antibody (Fig. 4*Ad*). TT demonstrated complete spermatogenesis with full mature sperm in the seminiferous tubules (Fig. 4*Ae*). That spermatogenesis originated from the EGFP-AP$^+$GSCs was further confirmed by anti-EGFP immunostaining. The significant EGFP-positive immunostaining of cells in the seminiferous tubules of TT is shown in Fig. 4*Af, g*. A negative control was produced using a control IgG as the primary antibody (Fig. 4*Ah*).

Next, the EGFP-AP$^+$GSCs were microinjected into blastocysts to test their pluripotent contribution to chimera offspring. Chimerism was observed in 76% (19 of 25) of the neonatal mice. EGFP-positive donor cells were found in the three germ layers of d 18 embryonic chimeras (Supplemental Fig. 3*Ba–l*) and colocalized with CD31 (mesoderm), cytokeratin-14 (ectoderm), and AFP proteins (endoderm) (Supplemental Fig. 2*Bm–o*). The d 4 neonatal chimeras were further subjected to IVIS for *in vivo* live fluorescence imaging. The GFP fluorescence was predominantly detected on the ventral side of the chimeras (Fig. 4*B*). The contribution of the EGFP$^+$AP$^+$GSCs in offspring seems not dominantly locate at skin and hair, although we still observed chimeric phenotype in the tail and dorsal/ventral sides (Fig. 4*C*, open arrowheads). However, by analyzing 3-wk-old chi-

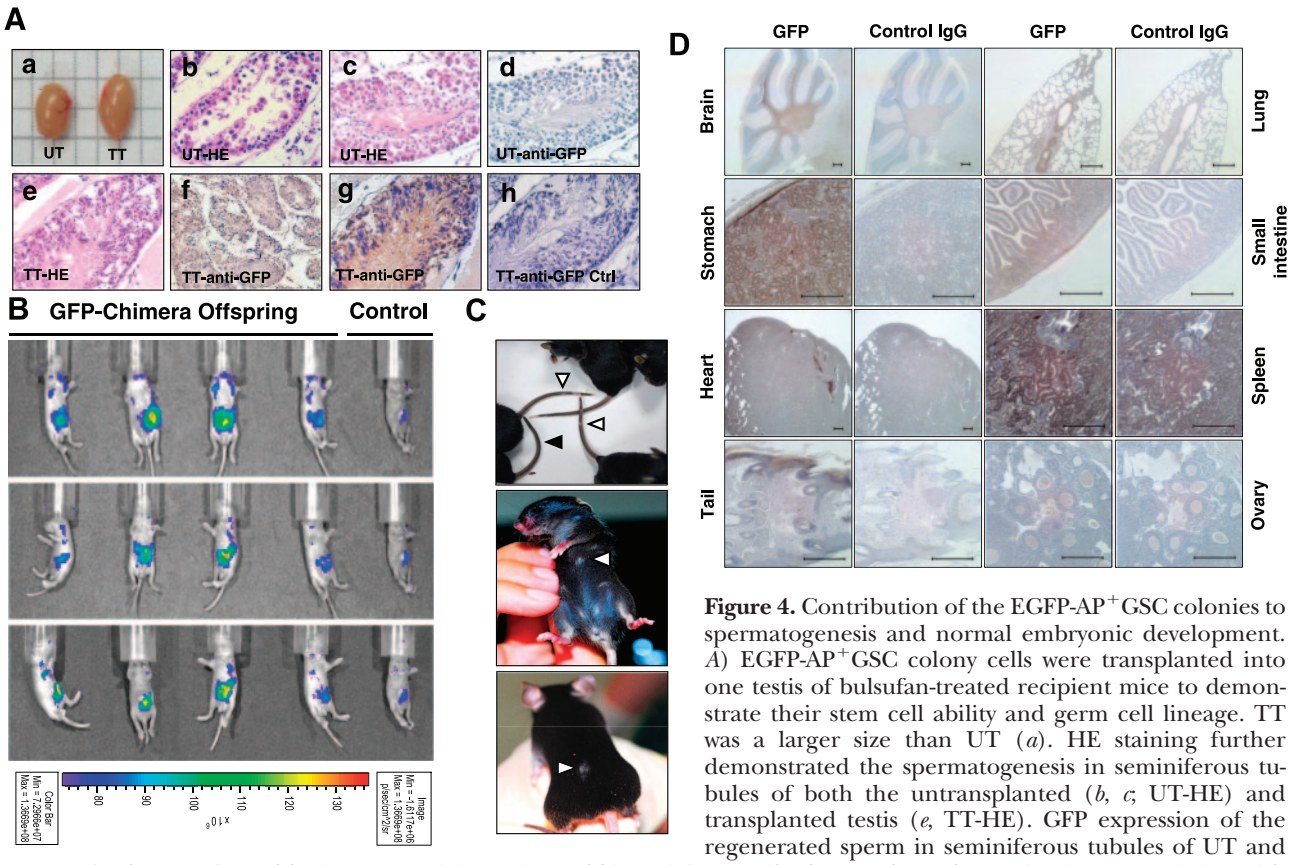

Figure 4. Contribution of the EGFP-AP$^+$GSC colonies to spermatogenesis and normal embryonic development. *A*) EGFP-AP$^+$GSC colony cells were transplanted into one testis of bulsufan-treated recipient mice to demonstrate their stem cell ability and germ cell lineage. TT was a larger size than UT (*a*). HE staining further demonstrated the spermatogenesis in seminiferous tubules of both the untransplanted (*b, c*; UT-HE) and transplanted testis (*e*, TT-HE). GFP expression of the regenerated sperm in seminiferous tubules of UT and TT was further confirmed by immunostaining using rabbit anti-GFP antibody. UT showed negative immunostaining with anti-GFP antibody (*d*); TT showed positive immunostaining (brown) with anti-GFP antibody (*f*, low magnification; *g*, high magnification). Rabbit IgG was used as a negative control (*h*, TT-anti-GFP Ctrl). *B–D*) EGFP-AP$^+$GSC colony cells were transplanted into the C57BL/6 mice blastomeric embryo and then implanted into the uterus of 2.5 dpc pseudo-pregnant CByB6F1 female mice. Contribution of EGFP-AP$^+$GSCs (from FVB mice) in chimera offspring was further examined by IVIS noninvasive live imaging (for d 4 neonatal mice; *B*), chimeric phenotype (*C*), and EGFP immunostaining (for 3-wk mice; *D*). Day 4 GFP chimera offspring showed positive GFP fluorescence at the ventral side by *in vivo* live IVIS imaging (*B*; 12/12). Nonchimeric neonatal mice served as a negative control (*B*). Chimeric phenotype of the 3-wk offspring was not dominantly expressed in skin and hair, but was evident in tail and ventral/dorsal sides (*C*; open arrowheads indicate chimera; solid arrowhead indicates wild-type). Contribution of EGFP-AP$^+$GSCs in 3-wk chimera offspring is shown in *D*. Positive EGFP immunostaining was recognized in brain, lung, stomach, small intestine, heart, spleen, tail, and weak expression in oocytes. IgG was used as control antibody. Scale bars = 200 μm.

mera mice, we found GFP-positive cells were observed in a wide variety of organs, including brain, lung, stomach, small intestine, heart, spleen, and tail. A small amount of the GFP-positive cells could be found in ovary (Fig. 4*D*). The teratoma formation ability of the AP$^+$GSCs was further examined by using NOD/SCID mice. The AP$^+$GSCs contributed some of the embryonic germ layers, such as muscle, adipose tissue, salivary-like cells, and CK-14$^+$ epithelial-like cells (Supplemental Fig. 4). Together with these observations it is suggested that AP$^+$GSCs derived from the serum-free testicular stromal coculture system exhibited the pluripotency.

Endocrine effect of IGF-1 on the formation of AP$^+$GSC colonies

The serum-free testicular stroma coculture system seems to provide microenvironmental factors that regulated the self-renewal growth and pluripotent status of AP$^+$GSCs. To uncover the microenvironmental factors that regulated the pluripotency of AP$^+$GSCs, cytokine antibody array was utilized to find the potential niche cytokine. As shown in **Fig. 5*A***, the AP$^+$GSC formation began on the third culture day and reached maximum with colony size and density at d 7. BM and D3-CM were collected and assayed for cytokine expression, which may activate the AP$^+$GSC formation. Figure 5*B* shows that several cytokines increased over time, most notably, IGF-1. To address the role of IGF-1 in AP$^+$GSC formation, increasing concentrations of IGF-1 were added to the medium in place of insulin. As shown in Fig. 5*C*, IGF-1 enhanced the colony formation in a dose-dependent manner at concentrations of 0–1 ng/ml. The IGF-1 effect reached a plateau at 1–10 ng/ml (with 80% of colony formation efficiency; $P<0.001$). This result not only demonstrates the dominant effect of IGF-1 on AP$^+$GSCs but also suggests the cooperative potential of IGF-1/IGF-1R with other receptor-mediated signaling pathways.

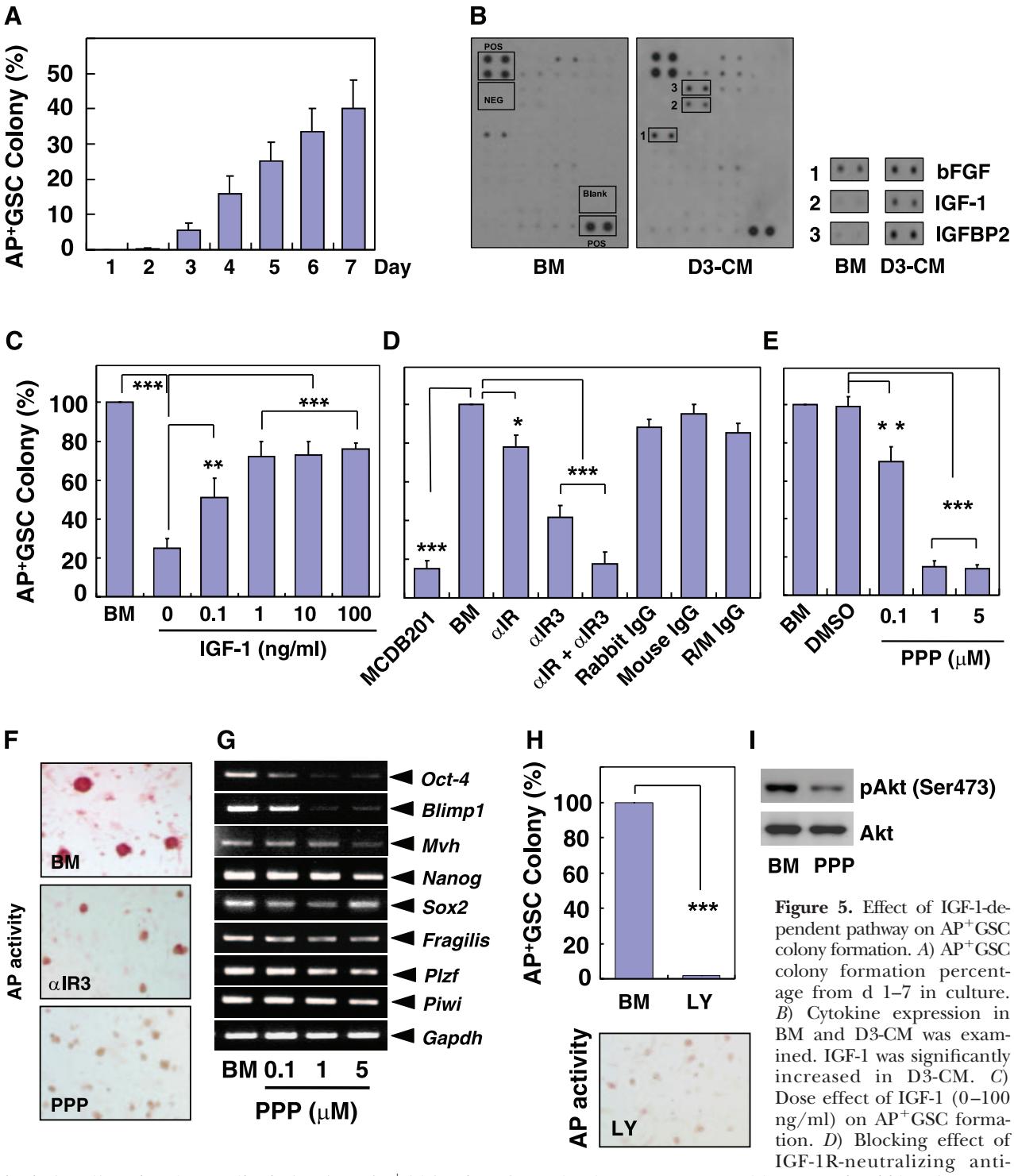

Figure 5. Effect of IGF-1-dependent pathway on AP$^+$GSC colony formation. *A*) AP$^+$GSC colony formation percentage from d 1–7 in culture. *B*) Cytokine expression in BM and D3-CM was examined. IGF-1 was significantly increased in D3-CM. *C*) Dose effect of IGF-1 (0–100 ng/ml) on AP$^+$GSC formation. *D*) Blocking effect of IGF-1R-neutralizing antibody (αIR3) and anti-IR antibody (αIR) on AP$^+$GSC colony formation in BM. BM was positive control; rabbit IgG, mouse IgG, and MCDB-201 served as negative controls. *E*) Blocking effect of PPP (IGF-1R blocker) in concentration of 0–5 μM on AP$^+$GSC colony formation in BM. BM, BM only; DMSO, DMSO-containing BM; PPP, PPP/DMSO-containing BM. *F*) AP activity and cell morphology of AP$^+$GSC colonies under αIR3 or PPP treatment. *G*) Effect of PPP on gene expression of AP$^+$GSC colony cells. *H*) Effect of LY294002 (a specific PI3K inhibitor; 10 μM) on colony formation and AP activity of AP$^+$GSCs. *I*) Western blotting shows Akt phosphorylation (Ser-473 of the AP$^+$GSCs was enhanced in BM, and significantly suppressed by the addition of PPP. Data are means ± SD of at least 3 independent determinations for each condition. *$P <$ 0.05; **$P < 0.01$, ***$P < 0.001$.

The important potential of IGF-1/IGF-1R-mediated signaling for the AP$^+$GSC colony formation was further supported by the insulin-containing medium we used in the cultures. In our experiments, by dissecting the medium components, we found insulin (5 μg/ml) significantly increased the percentage of AP$^+$GSC formation while compared with MCDB201 medium (Supplemental Fig. 5*A*; $P<0.001$). As insulin is known to activate both the

IR and the IGF-1R in a dose-dependent fashion, the dose effect of insulin on AP$^+$GSC colony formation was examined. As shown in Supplemental Fig. 5*B*, insulin increased the formation of AP$^+$GSCs at concentrations of 50 ng/ml to 5 μg/ml, which is much higher than its ligand affinity. This observation hints at the action of insulin on IGF-1R and strongly supports the premise that IGF-1/IGF-1R-mediated signaling is important for AP$^+$GSC colony formation.

The specific role of IGF-1 and insulin on AP$^+$GSC formation was further examined by using neutralizing antibody against IGF-1R (αIR3) and anti-IR (αIR). As shown in Fig. 5*D*, αIR3 specifically decreased the AP$^+$GSC formation ($P<0.001$). The αIR showed a slight suppression effect (~20%; $P<0.05$). The effect of IGF-1/IGF-1R on the AP$^+$GSC formation was further confirmed by using PPP treatment, which is known to selectively inhibit tyrosine-phosphorylation of IGF-1R and hence to suppress downstream signaling (18). As shown in Fig. 5*E, F*, PPP treatment not only affected the formation of AP$^+$GSC colony but also significantly suppressed the AP activity of these cells ($P<0.001$). Moreover, treatment of PPP significantly down-regulated the expression of *Oct-4, Nanog,* and *Sox2*, suggesting that IGF-1R-mediated signaling is important for maintaining the pluripotency of cultured SSCs. In addition, genes related to PGCs (such as *Blimp1, Mvh,* and *Fragilis*) and genes associated with self-renewal regulation (*e.g.*, *Plzf* and *Piwi*) were reduced (Fig. 5*G*). To further examine the possible signaling pathway responsible for AP$^+$GSC colony formation, the specific PI3K inhibitor LY294002 was used to block the IGF-1/IGF-1R-mediated signal pathway. As shown in Fig. 5*H*, LY294002 significantly suppressed GSC colony formation and AP activity of the AP$^+$GSCs. Akt phosphorylation (Ser-473 of the AP$^+$GSCs) was also dramatically suppressed by PPP treatment (Fig. 5*I*). Taken together, these findings strongly support the essential role of IGF-1/IGF-1R-mediated signaling is important for maintaining the stemness of SSCs.

Expression of IGF-1 by testicular stromal cells

To further identify the specific type of stromal cells responsible for producing IGF-1 to the culture, antibodies specifically against various types of testicular stromal cells were used including antibodies against myoid cells (anti-αSMA), Leydig cells (anti-CYP11A1), and Sertoli cells (anti-MIS). The results indicate laminin-coating apparently selectively adheres myoid cells and Leydig cells, which serve as feeder cells in AP$^+$GSC cultures. Most of the AP$^+$GSC colonies were closely associated with myoid cells (Supplemental Fig. 6), but the Leydig cells were responsible for producing IGF-1 to the culture, as expression of IGF-1 was obtained in Leydig cells, as judged by positive immunostaining results. As shown in **Fig. 6*Ac***, the expression of IGF-1 can be detected within Leydig cells (Fig. 6*Ad*, yellow). Furthermore, it seems that low-level expression of IGF-1 protein was also detected in the AP$^+$GSCs (Fig. 6*Ba*, arrows). The expression of *Igf-1* mRNA in individual AP$^+$GSC colonies is shown in the inset of Fig. 6*Ba*. Myoid cells showed negative immunostaining for IGF-1 expression (Fig. 6*Ba, b*; open arrowhead). In support of this observation, IGF-1 was positively detected in Leydig cells (solid arrowhead) and weakly in the seminiferous tubules (open arrowhead) in testis of d 0–2 neonatal mice (Fig. 6*Bc*). The positive and negative controls of the antibodies used for immunostaining of Fig. 6 are

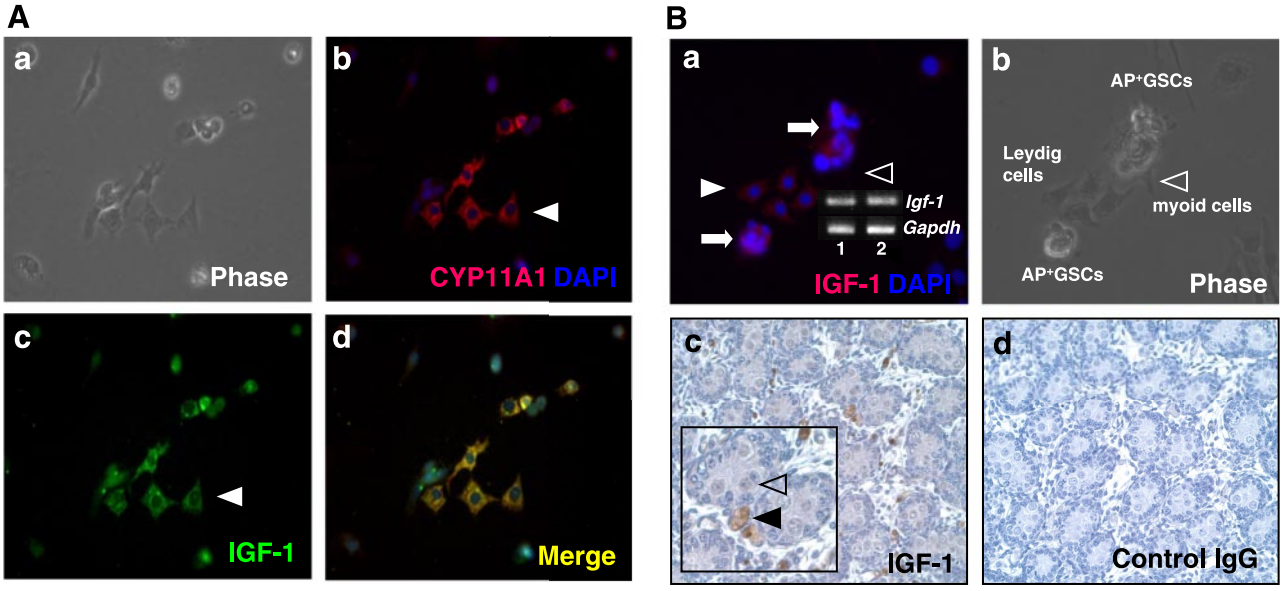

Figure 6. Expression of IGF-1 in Leydig cells and AP$^+$GSC colonies. *A*) Images show phase (*a*) and expression of IGF-1 (*c*, green) in Leydig cells (*b*, red), and colocalization (*d*, yellow). *B*) *a*) Expression of IGF-1 in Leydig cells (red; solid arrowhead) and AP$^+$GSCs (red; arrows). Inset: *igf-1* mRNA expression of each individual AP$^+$GSC. Open arrowhead indicates myoid cells. *Gapdh* was internal control. *b–d*) Phase image (*b*) and IGF-1 expression in interstitial space (solid arrowhead) and seminiferous tubules (open arrowhead) (*c*); rabbit IgG was negative control (*d*).

shown in Supplemental Fig. 7. The expression of IGF-1R and IR in AP^+GSCs was also confirmed by RT-PCR and immunocytochemical staining (Supplemental Fig. 8).

DISCUSSION

Germ cell pluripotency has been demonstrated by biological and experimental teratoma formation (2–4). However, little is known about the endocrine regulation of germ cell pluripotency. This lack of understanding leads to low efficiency when generating multipotent mouse GSCs from wild-type testis *in vitro* (3). In this report, we utilized a serum-free culture system and d 0–2 neonatal mice in which the testicular germ cells were in the gonocyte stage, to generate pluripotent stem cells from wild-type mouse testis. With this system, we found that IGF-1 secreted by Leydig cells may mediate IGF-1/IGF-1R through PI3K/Akt signaling to regulate pluripotent transcription factors such as *Oct-4* and germ cell pluripotency.

Many researchers have used serum-containing medium to cultivate GSCs and SSCs (3, 4, 6, 7); however, the detrimental effects of serum on the expansion of GSCs have also been reported (8, 19). In serum-free medium, MEF or STO cells have been commonly used as feeders to support the maintenance or proliferation of SSCs *in vitro* (6, 8, 19). Exogenous factors such as GDNF, bFGF, and/or GFRα1 have been regularly added to medium to support the SSC proliferation. In these experiments, some of the SSCs showed weak AP activity (8), c-$kit^+$$SSEA1^-$ (6), or chain formation (20). As stem cells are able to change their cell fate by quickly responding to their microenvironment, the complex serum components and nonphysiological feeders (MEF and/or STO cells) may dramatically hinder the pluripotent processes *in vitro* as well as hinder the identification of key endocrine factors involved in the regulation of GSC stemness.

In our experiment, the stem cell colonies showed strong AP activity (AP^+GSCs), in contrast to SSCs (3, 8). The AP^+GSC colonies showed clump morphology with no chain formation. This phenomenon is coincident with the very weak expression of *Tex 14* (Fig. 1*C*) located at the cytoplasmic bridges of A_{pair} or $A_{aligment4–32}$ cells of type A spermatogonia (10). With serum treatment, the AP^+GSC colony cells changed morphology to become flattened and expressed genes of differentiated sperm, including *Tex14, Dazl,* and *c-kit* (Supplemental Fig. 9). This result is consistent with a previous study that demonstrated a negative effect of serum on mouse SSC formation (8). The AP^+GSC colonies expressed SSEA-1 protein (Fig. 1*B*) (21) and shared some characteristics with ESCs/PGCs. For example, these colonies expressed *Oct-4* (*Pou5f1*) (22), *Nanog* (23), *E-ras* (24), and *Sox2* (25) in a manner similar to ESCs. *Nanog* is known to be expressed in ESCs but not SSCs (26). The expression of *Nanog* in AP^+GSCs strongly supports their pluripotent potential. The AP^+GSCs also showed PGC-like gene expression, including expression of *Oct-4*, *Sox2*, *Fragilis*, and *Stella* (27), *Blimp1* (B-lymphocyte-induced maturation protein-1) (28), and *Mvh* (Fig. 1*C*). The phenomenon of PGC migration (with AP positive staining) and trans-retinoic acid stimulated cell proliferation in the AP^+GSC colonies was also observed (Fig. 2*B*). The pluripotency of the AP^+GSC colonies was further demonstrated by their *in vitro* differentiation capacity (Fig. 3). In addition, the EGFP-AP^+GSCs showed the ability of teratoma-like formation by using NOD/SCID mice model and contributed to the three germ layers of the chimeras offspring by *in vivo* blastocyst injection (Fig. 4; Supplemental Figs. 3 and 4). Apparently, these primitive AP^+GSCs ($Oct\text{-}4^+$$c\text{-}kit^-$ GSCs) in neonatal testis were not limited to germ cell differentiation but also underwent dedifferentiation to become ES-like pluripotent stem cells.

Stromal cells that control the GSC fates in a culture environment were selected by coating material. In contrast to our previous study of lung stem cells, in which collagen I was the preferred substrate (29), laminin (at 275 ng/cm^2) was the optimal coating material to support AP^+GSC colony formation (Supplemental Fig. 1) and PGC-like migration (Fig. 2*B*). In support of these results, laminin has been shown to play an important role in PGC migration (30). Further examination by immunostaining demonstrated that laminin selected Leydig cells and myoid cells as feeders in our culture system (Supplemental Fig. 6; Fig. 6*A*). These cells may provide essential endocrine components, in addition to exogenous factors, that support the formation of pluripotent AP^+GSCs. Cytokine antibody arrays identified IGF-1 as an important factor (Fig. 5). This observation is consistent with our culture condition, which used insulin at a concentration of 5 μg/ml in medium. At this concentration, insulin is able to bind to the IGF-1R as well as the IR. In line with that, our data suggested an effective response on AP^+GSC colony formation at low concentrations of IGF-1 (1 ng/ml; Fig. 5*C*). The IGF-1 may be secreted from Leydig cells (31) and AP^+GSCs (Fig. 6*B*). As the AP^+GSCs express both the IR and IGF-1R at the gene and protein levels (Supplemental Fig. 8), the IGF-1 may interact with IGF-1R on the AP^+GSCs *via* a paracrine and/or autocrine manner to support the stemness of GSCs. This hypothesis is strongly supported by the positive immunohistochemical staining of IGF-1 in interstitial spaces and seminiferous tubules (Fig. 6*Bc*, *d*). Myoid cells are known to physiologically locate at the basal membrane and to be in close contact with the SSCs in testis. Leydig cells are located in the interstitial space close to myoid cells. The proximity of Leydig cells and myoid cells to basal membrane SSCs *in vivo* may govern the paracrine regulation of IGF-1 on SSC stemness. This hypothesis is strongly supported by a recent study by Oatley and Brinster (26), which suggests paracrine regulation of testicular interstitial space in germ cell stemness.

The IGF-1/IGF-1R-mediated signals in AP^+GSC formation was further verified by an antibody neutralizing assay and PPP treatment (Fig. 5*E*). PPP is known to efficiently inhibit the phosphorylation of IGF-1R without interfering with IR activity (18). The suppressive effect of PPP on formation of AP^+GSC colonies is consistent with the neutralizing effect of αIR3 (IGF-1R-neutralizing antibody). Most importantly, the pluripotent genes of the AP^+GSCs, such as *Oct-4*, *Blimp1*, *Sox2*, and *Nanog*, were dramatically suppressed by PPP, suggesting the IGF-1/IGF-1R-mediated signaling pathway in the regulation of the AP^+GSC pluripotency. IGF-1/IGF-1R is known to transmit intracellular signaling through PI3K/Akt or Ras/ERK pathway (32). In our experiments, the colony formation efficiency and AP activity of the AP^+GSCs were also dramatically reduced by LY294002 (Fig. 5*H*) but not by PD98059 (data not shown). In addition, the Akt phosphorylation (Ser-473 of AP^+GSCs was also dramatically suppressed by PPP (Fig. 5*I*). This observation strongly supports the association of IGF-1/IGF-1R-mediated PI3K/Akt signaling in AP^+GSC pluripotency. In line with our observations, recent studies (33, 34) have shown a close association between the PI3K-Akt pathway and the pluripotency of germ cells. Activation of the PI3K-Akt pathway in PGCs promotes cell proliferation as well as the conversion into teratoma or pluripotent embryonic germ cells. In addition, the PI3K/Akt signal axis has been shown to crosstalk with self-renewal mechanisms in ESCs (35, 36). In ESCs, IGF-1 has also been reported to cooperate with bFGF in the self-renewal process of ESCs (37). Similar to this observation, our results by cytokine array analysis demonstrated that the expression of IGF-1 and bFGF were increased in our culture medium for AP^+GSC formation (Fig. 5*B*). These results strongly support the role of IGF-1/IGF-1R signaling in the regulation of pluripotency of mouse GSCs.

The endocrine factors in the stroma cell microenvironment apparently play important roles in the regulation of germ cell pluripotency. The most important finding of our study was elucidating the role of endocrine factor IGF-1 and IGF-1/IGF-1R-mediated PI3K/Akt signaling in the regulation of mouse SSC stemness. This finding may have important implications in the study of endocrinology, germ cell development, and tumorigenesis. FJ

We thank Professor John Yu at the Stem Cell Program, the Genomics Research Center, Academia Sinica for encouragement and support. We also thank Ping Wu and Shu-Fen Cheng at the Department of Biochemistry and Dr. Chien-Jui Cheng at the Department of Pathology, Graduate Institute of Medical Sciences, Taipei Medical University, for excellent technical support. This work was supported by grants from the National Science Council, Taiwan, NSC93-2311-B-038-006, NSC95-2311-B-038-002-MY2, and NSC96-3111-B-038-001.

REFERENCES

1. De Rooij, D. G., and Grootegoed, J. A. (1998) Spermatogonial stem cells. *Curr. Opin. Cell Biol.* **10,** 694–701
2. Stevens, L. C. (1984) Spontaneous and experimentally induced testicular teratomas in mice. *Cell Differ.* **15,** 69–74
3. Kanatsu-Shinohara, M., Inoue, K., Lee, J., Yoshimoto, M., Ogonuki, N., Miki, H., Baba, S., Kato, T., Kazuki, Y., Toyokuni, S., Toyoshima, M., Niwa, O., Oshimura, M., Heike, T., Nakahata, T., Ishino, F., Ogura, A., and Shinohara, T. (2004) Generation of pluripotent stem cells from neonatal mouse testis. *Cell* **119,** 1001–1012
4. Guan, K., Nayernia, K., Maier, L. S., Wagner, S., Dressel, R., Lee, J. H., Nolte, J., Wolf, F., Li, M., Engel, W., and Hasenfuss, G. (2006) Pluripotency of spermatogonial stem cells from adult mouse testis. *Nature* **440,** 1199–1203
5. Barnes, D., and Sato, G. (1980) Serum-free cell culture: a unifying approach. *Cell* **22,** 649–655
6. Kanatsu-Shinohara, M., Miki, H., Inoue, K., Ogonuki, N., Toyokuni, S., Ogura, A., and Shinohara, T. (2005) Long-term culture of mouse male germline stem cells under serum-or feeder-free conditions. *Biol. Reprod.* **72,** 985–991
7. Nagano, M., Ryu, B. Y., Brinster, C. J., Avarbock, M. R., and Brinster, R. L. (2003) Maintenance of mouse male germ line stem cells in vitro. *Biol. Reprod.* **68,** 2207–2214
8. Kubota, H., Avarbock, M. R., and Brinster, R. L. (2004) Growth factors essential for self-renewal and expansion of mouse spermatogonial stem cells. *Proc. Natl. Acad. Sci. U. S. A.* **101,** 16489–16494
9. Oatley, J. M., Avarbock, M. R., Telaranta, A. I., Fearon, D. T., and Brinster, R. L. (2006) Identifying genes important for spermatogonial stem cell self-renewal and survival. *Proc. Natl. Acad. Sci. U. S. A.* **103,** 9524–9529
10. Hamra, F. K., Chapman, K. M., Nguyen, D., and Garbers, D. L. (2007) Identification of neuregulin as a factor required for formation of aligned spermatogonia. *J. Biol. Chem.* **282,** 721–730
11. Meng, X., Lindahl, M., Hyvönen, M. E., Parvinen, M., de Rooij, D. G., Hess, M. W., Raatikainen-Ahokas, A., Sainio, K., Rauvala, H., Lakso, M., Pichel, J. G., Westphal, H., Saarma, M., and Sariola, H. (2000) Regulation of cell fate decision of undifferentiated spermatogonia by GDNF. *Science* **287,** 1489–1493
12. Arighi, E., Borrello, M. G., and Sariola, H. (2005) RET tyrosine kinase signaling in development and cancer. *Cytokine Growth Factor Rev.* **16,** 441–467
13. Oatley, J. M., Avarbock, M. R., and Brinster, R. L. (2007) Glial cell line-derived neurotrophic factor regulation of genes essential for self-renewal of mouse spermatogonial stem cells is dependent on Src family kinase signaling. *J. Biol. Chem.* **282,** 25842–25851
14. Shen, C. N., Slack, J. M. W., and Tosh, D. (2000) Molecular basis of transdifferentiation of pancreas to liver. *Nat. Cell Biol.* **2,** 879–887
15. Brinster, R. L., and Avarbock, M. R. (1994) Germline transmission of donor haplotype following spermatogonial transplantation. *Proc. Natl. Acad. Sci. U. S. A.* **91,** 11303–11307
16. Horii, T., Nagao, Y., Tokunaga, T., and Imai, H. (2003) Serum-free culture of murine primordial germ cells and embryonic germ cells. *Theriogenology* **59,** 1257–1264
17. Koshimizu, U., Watanabe, M., and Nakatsuji, N. (1995) Retinoic acid is a potent growth activator of mouse primordial germ cells in vitro. *Develop. Biol.* **168,** 683–685
18. Girnita, A., Girnita, L., del Prete, F., Bartolazzi, A., Larsson, O., and Axelson, M. (2004) Cyclolignans as inhibitors of the insulin-like growth factor-1 receptor and malignant cell growth. *Cancer Res.* **64,** 236–242
19. Kubota, H., Avarbock, M. R., and Brinster, R. L. (2004) Culture conditions and single growth factors affect fate determination of mouse spermatogonial stem cells. *Biol. Reprod.* **71,** 722–731
20. Kanatsu-Shinohara, M., Ogonuki, N., Inoue, K., Miki, H., Ogura, A., Toyokuni, S., and Shinohara, T. (2003) Long-term proliferation in culture and germline transmission of mouse male germline stem cells. *Biol. Reprod.* **69,** 612–616
21. Solter, D., and Knowles, B. B. (1978) Monoclonal antibody defining a stage-specific mouse embryonic antigen (SSEA-1). *Proc. Natl. Acad. Sci. U. S. A.* **75,** 5565–5569
22. Nichols, J., Zevnik, B., Anastassiadis, K., Niwa, H., Klewe-Nebenius, D., Chambers, I., Schöler, H., and Smith, A. (1998) Formation of pluripotent stem cells in the mammalian embryo depends on the POU transcription factor Oct4. *Cell* **95,** 379–391
23. Mitsui, K., Tokuzawa, Y., Itoh, H., Segawa, K., Murakami, M., Takahashi, K., Maruyama, M., Maeda, M., and Yamanaka, S.

(2003) The homeoprotein nanog is required for maintenance of pluripotency in mouse epiblast and ES cells. *Cell* **113,** 631–642
24. Takahashi, K., Mitsui, K., and Yamanaka, S. (2003) Role of ERas in promoting tumour-like properties in mouse embryonic stem cells. *Nature* **423,** 541–545
25. Pan, G., and Thomson, J. A. (2007) Nanog and transcriptional networks in embryonic stem cell pluripotency. *Cell Res.* **17,** 42–49
26. Oatley, J. M., and Brinster, R. L. (2008) Regulation of spermatogonial stem cell self-renewal in mammals. *Annu. Rev. Cell Dev. Biol.* **3,** 263–286
27. Saitou, M., Barton, S. C., and Surani, M. A. (2002) A molecular programme for the specification of germ cell fate in mice. *Nature* **418,** 293–300
28. Ohinata, Y., Payer, B., O'Carroll, D., Ancelin, K., Ono, Y., Sano, M., Barton, S. C., Obukhanych, T., Nussenzweig, M., Tarakhovsky, A., Saitou, M., and Surani, M. A. (2005) Blimp1 is a critical determinant of the germ cell lineage in mice. *Nature* **436,** 207–213
29. Ling, T. Y., Kuo, M. D., Li, C. L., Yu, A. L., Huang, Y. H., Wu, T. J., Lin, Y. C., Chen, S. H., and Yu, J. (2006) Identification of pulmonary Oct-4+ stem/progenitor cells and demonstration of their susceptibility to SARS coronavirus (SARS-CoV) infection in vitro. *Proc. Natl. Acad. Sci. U. S. A.* **103,** 9530–9535
30. García-Castro, M. I., Anderson, R., Heasman, J., and Wylie, C. (1997) Interactions between germ cells and extracellular matrix glycoproteins during migration and gonad assembly in the mouse embryo. *J. Cell Biol.* **138,** 471–480
31. Villalpando, I., Lira, E., Medina, G., Garcia-Garcia, E., and Echeverria, O. (2008) Insulin-like growth factor 1 is expressed in mouse developing testis and regulates somatic cell proliferation. *Exp. Biol. Med.* **233,** 419–426
32. Taniguchi, C. M., Emanuelli, B., and Kahn, C. R. (2006) Critical nodes in signalling pathways: insights into insulin action. *Nat. Rev.* **7,** 85–96
33. Moe-Behrens, G. H., Klinger, F. G., Eskild, W., Grotmol, T., Haugen, T. B., and De Felici, M. (2003) Akt/PTEN signaling mediates estrogen-dependent proliferation of primordial germ cells in vitro. *Mol. Endocrinol.* **17,** 2630–2638
34. Kimura, T., Suzuki, A., Fujita, Y., Yomogida, K., Lomeli, H., Asada, N., Ikeuchi, M., Nagy, A., Mak, T. W., and Nakano, T. (2003) Conditional loss of PTEN leads to testicular teratoma and enhances embryonic germ cell production. *Development* **130,** 1691–1700
35. McLean, A. B., D'Amour, K. A., Jones, K. L., Krishnamoorthy, M., Kulik, M. J., Reynolds, D. M., Sheppard, A. M., Liu, H., Xu, Y., Baetge, E. E., and Dalton, S. (2007) Activin a efficiently specifies definitive endoderm from human embryonic stem cells only when phosphatidylinositol 3-kinase signaling is suppressed. *Stem Cells* **25,** 29–38
36. Watanabe, S., Umehara, H., Murayama, K., Okabe, M., Kimura, T., and Nakano, T. (2006) Activation of Akt signaling is sufficient to maintain pluripotency in mouse and primate embryonic stem cells. *Oncogene* **25,** 2697–2707
37. Bendall, S. C., Stewart, M. H., Menendez, P., George, D., Vijayaragavan, K., Werbowetski-Ogilvie, T., Ramos-Mejia, V., Rouleau, A., Yang, J., Bossé, M., Lajoie, G., and Bhatia, M. (2007) IGF and FGF cooperatively establish the regulatory stem cell niche of pluripotent human cells in vitro. *Nature* **448,** 1015–1021

Received for publication September 25, 2008.
Accepted for publication January 29, 2009.